Iğdır Üniversitesi Fen Bilimleri Enstitüsü Dergisi, 14(3), 1218-1227, 2024
Journal of the Institute of Science and Technology, 14(3), 1218-1227, 2024
ISSN: 2146-0574, eISSN: 2536-4618
Chemistry **DOI: 10.21597/jist.1490644**
Research Article
Received: 27.05.2024 **Accepted: 14.06.2024**
To Cite: Canpolat, M. (2024). Effectively Removing Methyl Orange From Aqueous Solutions Using Sulphuric Acid Modified Midyat Stone. *Journal of the Institute of Science and Technology*, 14(3), 1218-1227.

Effectively Removing Methyl Orange From Aqueous Solutions Using Sulphuric Acid Modified Midyat Stone

Mutlu CANPOLAT

Highlights:
- Physical Chemistry
- Purification of wastewater
- Dye Removal

Keywords:
- Modified Midyat stone
- Adsorption
- Methyl orange
- Kinetic models
- Isotherm models

ABSTRACT:

In this research, the efficiency of Midyat stone modified with sulphuric acid (H_2SO_4) in the removal of Methyl Orange (MO) from wastewater is evaluated. Various factors such as contact time, initial MO concentration, and adsorbent dosage were investigated to understand their influence on adsorption efficiency. The optimal conditions for MO removal were as follows: initial concentration 300 mg/L, contact time 70 min, adsorbent dosage 0.5 g. The surface properties of modified Midyat stone (MMS) were investigated using methods such as Fourier transform infrared spectroscopy (FT-IR) and Brunauer, Emmett, and Teller (BET). According to the findings, the isotherm data agreed with the Langmuir isotherm model, indicating both chemical sorption and irreversibility potential. The adsorption capacity of MO at 298, 308 and 318 K was calculated to be 50.02, 54.05 and 58.48 mg/g, respectively. In addition, adsorption kinetics data supported the pseudo-second-order (PSO) kinetic model for MO removal. The research identified MMS as a capable and adaptable substance for capturing MO ions from the aqueous environment due to its significant removal capacity, easy availability, and cost-effectiveness.

[1]Mutlu CANPOLAT (**Orcid ID:** 0000-0002-3771-6737), Department of Chemistry and Chemical Processing Technologies, Vocational School of Technical Sciences, Batman University, Batman, Türkiye

***Corresponding Author:** Mutlu CANPOLAT, e-mail: mutlu.canpolat@batman.edu.tr

INTRODUCTION

Natural resources are rapidly depleting due to rapid developments in industry, urbanization, and population growth. As a result of this loss of resources, the quality of air and water deteriorates. Activities such as textile production, drug production, heavy metal use, and fertilization cause pollution of water resources. These pollutants pose significant threats to both the environment and human health (Ekinci, 2023; Pandey and Ramontja, 2016; Iwuozor et al., 2021; Liu et al., 2020). Under anaerobic conditions, dyes can emit toxic and carcinogenic metabolites. Physical and chemical treatment methods can be used to prevent dye pollution in the water environment; however, these methods are costly, and some of them may cause sludge production (Sayğılı et al., 2015; Hasanbeigi and Price, 2015; Zhul-quarantine et al., 2018; Onat and Ekinci, 2024). Alternative methods are required to remove the color of the wastewater. The treatment of pollutants in aqueous media is a well-known and influential process; in-depth research in this field continues. Methyl orange is an azo colorant with the chemical formula $C_{14}H_{14}N_3NaO_3S$ and is widely used as an acid-base indicator. It gives red color in acidic medium and yellow color in basic medium. Due to these properties, it is used in titration and chemical analyses. However, methyl rhodamine can be found in industrial wastes and can harm to the environment. It can cause toxicity in aquatic ecosystems, negatively affect biodiversity and cause colouration of water resources. Global efforts are underway to combat MO pollution, which is an urgent problem among environmental issues. For these reasons, the adsorption of MO from wastewater is of great importance. Several approaches have been created to combat the removal of colorants. Comparatively, adsorption has proven to be a more practical and advantageous method due to its effectiveness and cost-effectiveness in removing dyes (Güzel et al., 2015; Tural et al., 2017; Tamjidi et al. 2019; Ren et al. 2017). Researchers have looked into using different adsorbents to extract colors from wastewater (Zhul-quarnain et al., 2018; Tural et al., 2017; Kaushal et al. 2020). Utilizing different physical-chemical reactions, each adsorbent exhibits selectivity for specific dyes. There is a continuous search for new adsorbents that can reduce the concentration of dyes such as MO in aqueous solutions to permissible limits.

In recent years, the use of industrial wastes in the removal of dyestuffs has attracted great interest, primarily because of their affordability and minimal secondary waste production. Materials with $CaCO_3$ in their composition have the capacity to adsorb dyes (Canpolat, 2023; Teğin et al. 2023; Onursal et al. 2020). However, calcite in calcareous soils acts as an effective adsorbent for dyestuff ions and contributes positively to environmental metal removal processes (Altunkaynak, 2022; Kahvecioğlu et al. 2023). The build-up of stone fragments is a serious environmental issue for stone processing facilities, which continue to grow and increase their production capacity in line with the industry's growth, and increasing demand (Bakalár et al. 2023). Midyat stone, a whitish-yellow limestone variety, stands out for its easy cutting, drilling, carving and shaping. This natural quality makes it a popular choice for construction materials in the region's architectural projects, capitalizing on the stone's attractive properties.

This study examines the modification of effective Midyat stone (MMS) using sulfuric acid (H_2SO_4) and its subsequent application as an adsorbent to remove MO dye from wastewater. The research focuses on evaluating various parameters that influence the efficiency of MO removal, including the starting dye amount, temperature, interaction time, and dosage of adsorbent. Additionally, the study assesses the adsorption process's kinetics and isotherms, ultimately determining the adsorption capacity of the modified Midyat stone (MMS).

MATERIALS AND METHODS

The Midyat Stone (MS), employed as an adsorbent in this investigation, came from quarries in the Midyat district of Mardin's Barış Tepe area. The stone pieces were first crushed in a jaw crusher, then ground in a ball mill and sieved to reduce the particle size below 75 microns. To prepare the modified Midyat stone, 10 g MS was first dissolved in 50 mL aqueous solution containing 1 N H_2SO_4. After that, the mixture was agitated at room temperature for 24 hours. After the agitation, centrifugation was used to remove the modified Midyat stone (MMS) components from the mixture. The separated MMS was repeatedly purged with distilled water until the pH of the purged solution reached seven to guarantee the removal of residual acid and other contaminants. After final drying at 105°C, the MMS product was used in adsorption experiments.

A concentration of 1000 mg/L was prepared to create the MO stock solution for the adsorption investigation. The resulting stock solution was then used to produce the lower concentration MO solutions required for the investigation. Every adsorption study was carried out with freshly prepared dilutions. All chemicals used in the research were obtained from Sigma-Aldrich.

Adsorbent Description

Midyat stone's functional groups' binding behavior was examined using FTIR spectroscopy. Low temperature N_2 sorption measurements were used to calculate the specific surface area using BET analysis.

Adsorption study

Adsorption studies were conducted using 250 mL conical flasks with 100 rpm swirling. MO concentrations ranged from 50 to 500 mg/L. Subsequently, the bottles were agitated in a shaker equipped with time and temperature controls. After the combination had had time to acclimate, it was centrifuged. The amount of remaining unadsorbed MO was determined using UV-Vis Spectroscopy (Shimadzu-1900 model). The initial MO ion concentration and contact time were considered while calculating the optimal parameters for adsorption studies. The quantity of adsorbed MO ions was determined using equation (1) (Canpolat et al., 2023; Lima et al., 2020).

$$q_e = \frac{C_i - C_e}{W} V \quad (1)$$

Where C_i and C_e (mg/L) denote the starting and equilibrium concentrations of MO, the MO solution's volume is indicated by V (L), while the MMS's mass is indicated by W (g).

RESULTS AND DISCUSSION

FT-IR Analysis

Figure 1 displays the FTIR spectra of MS, MMS, and MMS-MO. The FTIR spectrum of MS was determined in our previous studies (Canpolat, 2023). In the FTIR spectrum of MS; 1415 1/cm out-of-plane stretching, 875 1/cm asymmetric stretching (degenerate) vibration bands and 726 1/cm plane bending (double degenerate) vibration bands prove the existence of the calcite. The positions and intensities of the peaks of these groups changed slightly after modification (1440, 878 and 722 1/cm) and after MMS and MO adsorption (1440, 878 and 722 1/cm).

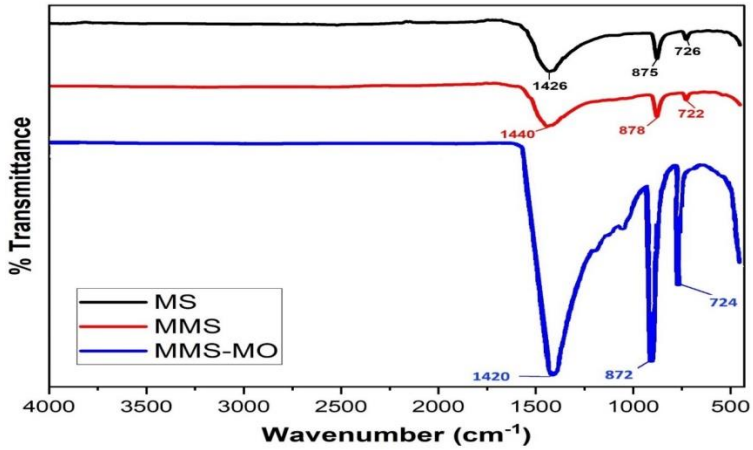

Figure 1. FTIR Spectra of MS, MMS and MMS-MO (after adsorption)

The impact of starting concentration

The solution's starting concentration has a significant impact on the adsorption process. In this investigation, potential changes in adsorption rates with adsorption time and initial concentration are indicated by kinetic parameters. To study this effect, solutions containing MO (from 50 to 500 mg/L) were prepared in volumes of 25 mL. These solutions were then combined with 0.5 g MMS and shaken for 120 minutes at 298, 308, and 318 K temperatures on a shaker. The amount of MO remaining in the solution after adsorption was then measured using a UV spectrophotometer. Every measure was made three times on the same or different days to ensure consistency. The resulting data averages were used for calculations. Figure 2 shows the correlation between the starting concentration and the removal of MO from wastewater by MMS. It was observed that as the MO concentration increased, the MO adsorption increased up to a certain concentration and remained constant after this concentration. This behavior is most likely caused by MO saturation of the MMS active sites. In light of these results, a 350 mg/L concentration of MO solution was chosen for the following stages of the study.

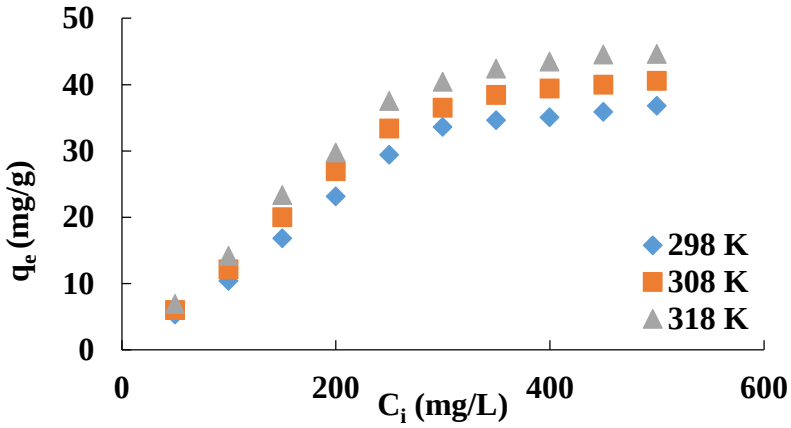

Figure 2. MMS was used to examine the effect of starting concentration on MO removal (0.5 g adsorbent mass, C_0 varying from 50 to 500 mg/L and V: 25 mL)

Contact time's impact

The duration of MO's solution-to-adsorbent contact is critical to the adsorption process. The equilibrium point of the MO solution at a 350 mg/L starting concentration was found to be 70 min, covering a range of temperature (298, 308, and 318 K) and time (10-120 min) (Figure 3). During the removal of MO, the elimination rate exhibited a sharp rise in the first phases due to the expansive area available. Subsequently, the removal rate slowed down when the surface of the sorbent reached saturation to reach equilibrium. As shown in Figure 3, the amounts of MO reaching equilibrium at a

350 mg/L starting concentration were calculated as 34.61, 38.43, and 42.35 mg/g for the respective operating temperatures. Furthermore, the information obtained from this study was used to evaluate the kinetics of the extraction procedure.

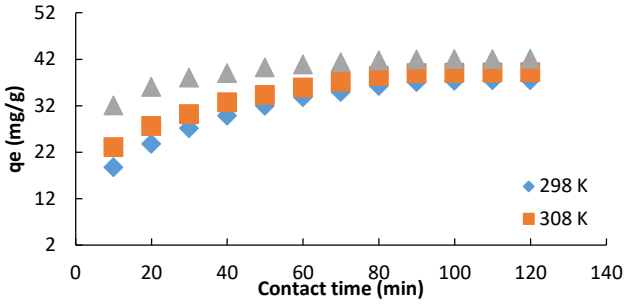

Figure 3. Contact time impacts on MO ion adsorption using MMS removal (0.5 g adsorbent mass, C_0: 500 mg/L, V: 25 mL)

Adsorbent's dosage effect

To evaluate the effect of the adsorbent amount, 350 mg/L MO (25 mL) was added to MMS in amounts ranging from 0.1 g to 1 g. In separate investigations carried out at 298 K with a stirring speed of 150 rpm for 120 min, it was found that the adsorption of MO ions onto MMS increased until the amount of adsorbent reached 0.5 g, after which it stabilized (Figure 4). This stabilisation is attributed to the existing adsorption sites' saturation. It was then determined that it would be appropriate to use 0.5 g MMS in the later stages of the study. This decision was based on the expectation that the adsorbent capacity would either remain consistent or decrease with further increases in the amount of adsorbent, rendering additional adsorbent ineffective.

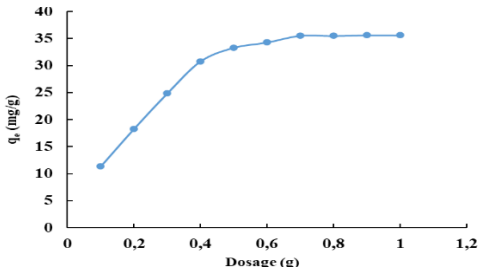

Figure 4. The impact of varying dosages on the adsorption of MO onto MMS

Kinetic study

Kinetic studies were performed to understand the mechanisms underlying the adhesion of MO ions to MMS and to determine the step in the process where the rate of progression is most limited. As shown in Figure 3, the adsorption capacity of MMS showed a rapid increase in the initial phase of the contact time. Within the first 70 min, a significant fraction of MO ions were adsorbed, attributed to the abundance of empty adsorption sites at shorter contact intervals. As the contact time increased, these empty sites were filled with target ions, causing the adsorption process to slow down gradually. For a more comprehensive understanding of the kinetic aspects, non-linear kinetic modelling was applied. Pseudo-First Order (PFO), Pseudo-Second Order (PSO) and Elovich kinetic models were used to analyse the adsorption data. The corresponding non-linear kinetic equations for PFO, PSO, Elovich, and Weber-Morris are given as Equations 2, 3, 4, and 5 (Akpomie et al., 2015; Altunkaynak, 2023; Altunkaynak and Canpolat, 2022; Canpolat and Topal, 2023).

$$\ln(q_e - q_t) = lnq_e - k_1 t \quad (2)$$

$$\frac{t}{q_t} = \frac{t}{q_e} + \frac{1}{k_2 q_e^2} \quad (3)$$

$$q_t = \frac{1}{\beta}\ln(\alpha\beta) + \frac{1}{\beta}\ln t \quad (4)$$

$$q_t = k_d t^{0.5} + C \quad (5)$$

In this context, 'q_t' refers the capacity for adsorption at time 't', while 'q_e' represents the cumulative amount of MO. The adsorption rate constants for PFO, and PSO are denoted by k_1 and k_2, where α denotes the initial adsorption rate. In addition, β represents the adsorption constant related to the surface coverage. Furthermore, K_d represents the reaction rate constant and C corresponds to the intersection point determined by the boundary layer thickness formed.

Table 1 and Figure 5 show the kinetic parameters that were derived from the models' non-linear graphs. According to Table 1, the q_e values over time can be determined for temperatures of 298, 308 and 318 K. The relatively high R^2 coefficients as well as the q_{max} values calculated with respect to the experimental counterparts indicate that the PSO model effectively characterises the kinetics of MO ion adsorption on MMS. Temperature-dependent increases in the computed k_2 values imply a temperature-dependent relationship in the processes.

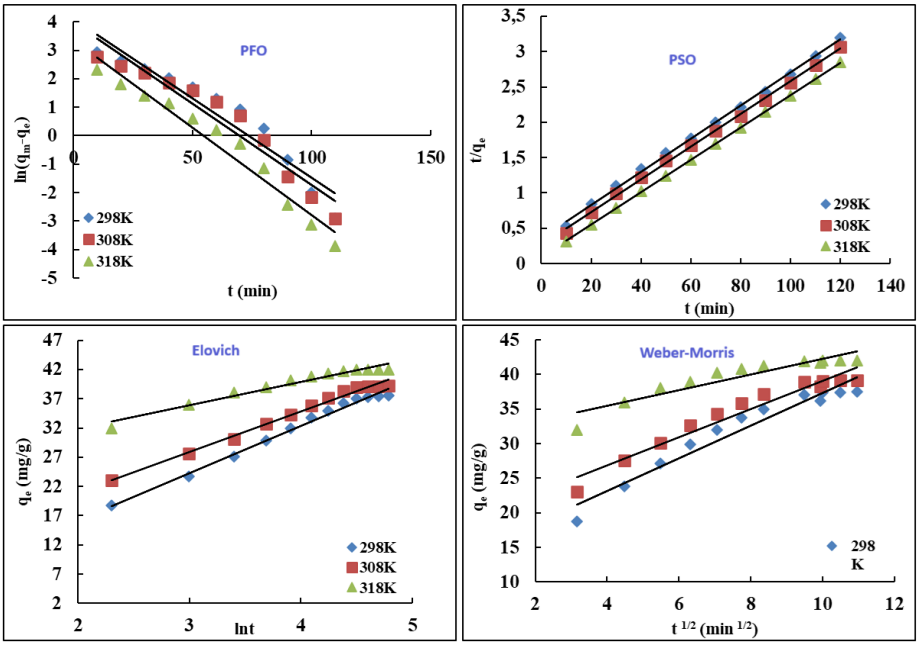

Figure 5. For the MO adsorption onto MMS, the kinetic model graphs

Table 1. Kinetic constants for the elimination of MO with MMS

	PFO				PSO			
(K)	*Line Eq.*	R^2	k_1	*qm*	*Line Eq.*	R^2	k_2	*qm*
298	y=-0.0559x + 4.1156	0.9215	0.0559	61.29	y=0.0234x + 0.3661	0.9984	0.0015	42.74
308	y=-0.0569x + 3.9759	0.9338	0.0569	53.30	y=0.0231x + 0.2647	0.9986	0.0020	43.29
318	y=-0.0614x + 3.3735	0.9586	0.0614	29.18	y=0.0229x + 0.0955	0.9999	0.0055	43.67
Weber- Morris					**Elovich**			
(K)	*Line Eq.*	R^2	K_d	C_b	*Line Eq.*	R^2	*β*	*α*
298	y= 2.3592x+13.764	0.9444	2.3592	13.764	y=8.0885x+0.0472	0.9899	0.124	8.112
308	y= 2.0364x+18.749	0.9463	2.0364	18.749	y=6.9697x+6.9581	0.9885	0.143	18.91
318	y= 1.1404x+30.867	0.8667	1.1404	30.867	y=4.0211x+23.795	0.9609	0.249	1503.1

Adsorption isotherms study

An investigation was conducted to find out how the concentration of MO ions influences adsorption, based on the findings displayed in Figure 1. As MO concentrations increased, the initial removal rate decreased, and this was explained by the MMS surface being saturated. Once equilibrium was attained, the removal rate did not change.

MMS used four isotherm equations (Equations 6-9) to evaluate the elimination of MO (Altunkaynak et al., 2022; Kara et al., 2018).

The Langmuir model is expressed as in equation 6.

$$\frac{C_e}{q_e} = \frac{1}{qmax.K_L} + \frac{C_e}{qmax} \quad (6)$$

The symbol K_L stands for the adsorption constant.

All of the molecular interactions that occur between the adsorbent and adsorbate are considered by the Freundlich isotherm model.

$$logq_e = logK_F + (1/n)logC_e \quad (7)$$

Here, n and K_F represent the intensity and adsorption capacity, respectively.

The D-R model is expressed as in equation 8.

$$Inq_e = Inq_{max} - K_{DR}\varepsilon^2 \quad (8)$$

K_{DR} is the equilibrium constant in the equation, while ε is the Polanyi.

The Temkin model is expressed as in equation 9.

$$q_e = \frac{RT}{b_T} + \ln(K_T C_e) \quad (9)$$

The equilibration constant in this case is represented by K_T, and the heat of adsorption by b_T. Table 2 provides a full breakdown of the variables that depend on adsorption, and Figure 6 displays the graphs that show the adsorption isotherms.

Two basic adsorption mechanisms, physical and chemical, can be defined based on the bonds that develop between the adsorbed material and the adsorbent. Adsorption equilibrium data for MO ions are shown in Figure 6. Table 2 summarizes the isotherm parameters that were computed. When Table 2 is analyzed, it becomes clear that the Langmuir model stands out as the most suitable isotherm model for MO adsorption and proves the possibility of chemical adsorption and the potential irreversibility of the process. Under the assumption of valid Langmuir conditions, the maximum removal capacity of MO on MMS was determined as 50.02, 54.05 and 58.48 mg/g at temperatures of 298, 308, and 318 K, respectively. This implies a monolayer coating of MMS, indicating a commendable adsorption capacity for MO ions.

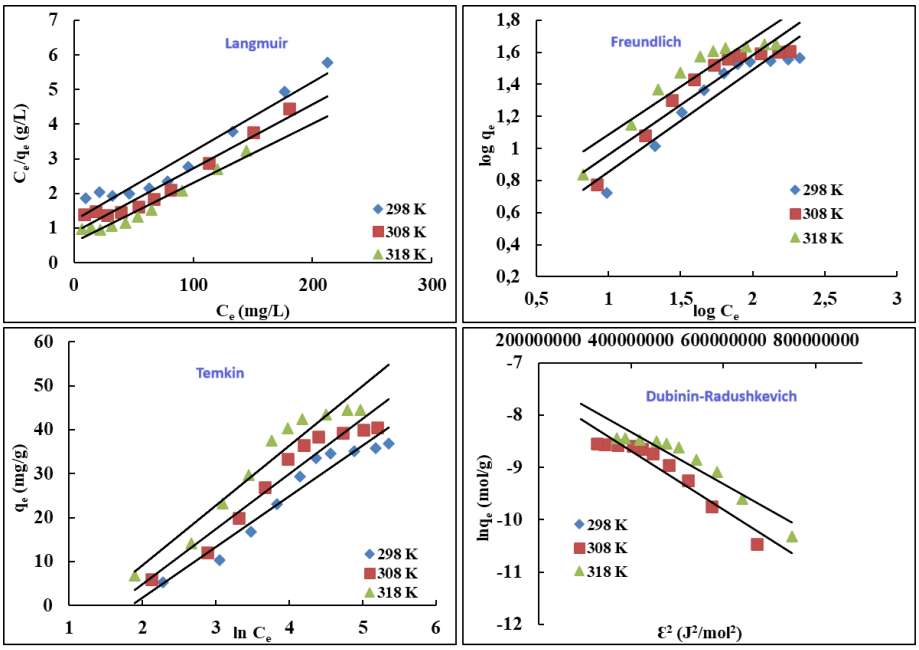

Figure 6. The adsorption of MO ions onto MMS is represented by isotherm models

Table 2. Adsorption of MO Ions on MMS: Isotherm Parameters

	Constants	298 K	308 K	318 K
Langmuir	K_L(L/mg)	0.0164	0.0213	0.0290
	$q_{max.}$ (mg/g)	50.02	54.05	58.48
	R^2	0.9456	0.9514	0.9594
Freundlich	n	1.57	1.61	1.67
	K_f	1.65	2.20	3.07
	R^2	0.8907	0.8798	0.8758
Temkin	A_T (L/g)	0.157	0.199	0.264
	b_T (j/mol)	215.07	204.01	194.06
	R^2	0.9365	0.9396	0.9861
D-R	K_{DR}	6.10^{-9}	5.10^{-9}	5.10^{-9}
	E(kj/mol)	9.13	10	10
	R^2	0.9216	0.8527	0.9084

Desorption studies

Enhancing the separation processes' economics through material regeneration is crucial. It is possible to employ a material with strong desorption potential in later adsorption processes. To verify reusability, experiments were conducted using MO-loaded MMS with identical experimental settings. The analytical materials were loaded with preset MO concentrations, washed with 250 mL of pure water, and dried for 24 hours at 80 °C in an oven. After that, the components were put in 100 milliliters of 0.1 mol/L NaOH to remove MO. Its stability and reusability were assessed by repeating four consecutive tests. The adsorbent was dried at 80 °C for one hour before being reused, and it was soaked in 0.1 mol/L NaOH after each cycle. Table 3 demonstrates that MMS demonstrated a strong MO removal capacity throughout four cycles.

Table 3. Desorption results

Adsorbent	Adsorbate	Cycle 1	Cycle 2	Cycle 3	Cycle 4
MMS	MO	92.4%	86.3%	67.4%	52.2%

CONCLUSION

In this study, waste Midyat stone was modified with H_2SO_4 and applied as an adsorbent for removing MO from wastewater. Remarkably, MMS exhibited an impressive removal efficiency for MO ions (50.02 mg/g at 298 K, 54.05 mg/g at 308 K, and 58.48 mg/g at 318 K). The equilibrium investigation showed that the Langmuir model provided a superior fit to the system. Kinetic investigations showed that the removal of MO was by the PSO equation. FT-IR and BET analyses confirmed that the MMS showed visible differences before and after the removal process. These structural and morphological changes suggest that adsorption and sedimentation reactions contribute significantly to the mechanism of MO removal from aqueous solutions. Considering the data, it can be concluded that Midyat stone shows efficiency and economic viability as a solution for the removing of MO from wastewater due to its abundant availability, significant adsorption capacity and cost effectiveness.

Conflict of Interest

The author of the article declares that he has no conflict of interest.

REFERENCES

Akpomie, K. G., Dawodu, F. A., & Adebowale, K. O. (2015). Mechanism on the sorption of heavy metals from binary-solution by a low cost montmorillonite and its desorption potential. *Alexandria Engineering Journal*, 54(3), 757-767.

Altunkaynak, Y. (2022). Effectively removing Cu (II) and Ni (II) ions from aqueous solutions using chemically non-processed Midyat stone: equivalent, kinetic and thermodynamic studies. *Journal of the Iranian Chemical Society*, 19(8), 3357-3370.

Altunkaynak, Y. (2023). Using chemically unprocessed orange peel to effectively remove Hg (II) ions from aqueous solutions: equivalent, thermodynamic, and kinetic investigations. *Sakarya University Journal of Science*, 27(1), 189-203.

Altunkaynak, Y., & Canpolat, M. (2022). Ham Portakal Kabuğu ile Sulu Çözeltilerden Mangan (II) İyonlarının Uzaklaştırılması: Denge, Kinetik ve Termodinamik Çalışmalar. *Afyon Kocatepe Üniversitesi Fen Ve Mühendislik Bilimleri Dergisi*, 22(1), 45-56.

Altunkaynak, Y., Canpolat, M., & Aslan, M. (2023). Adsorption of lead (II) ions on kaolinite from aqueous solutions: isothermal, kinetic, and thermodynamic studies. *Ionics*, 29(10), 4311-4323.

Bakalár, T., Kaňuchová, M., Girová, A., Pavolová, H., Hromada, R., & Hajduová, Z. (2020). Characterization of Fe (III) adsorption onto zeolite and bentonite. *International Journal of Environmental Research and Public Health*, 17(16), 5718.

Canpolat, M. (2023). Removing Co (II) and Mn (II) ions effectively from aqueous solutions by means of chemically non-processed Mardin stone waste: Equivalent, kinetic, and thermodynamic investigations. *Environmental Progress & Sustainable Energy*, 42(3), e14042.

Canpolat, M., & Topal, G. (2023). Synthesis, characterization of cross-linked poly (ethylene glycol dimethacrylate-methyl methacrylate-N-(1-phenylethyl) acrylamide) copolymer and removal of copper (II), cobalt (II) ions from aqueous solutions via this copolymer. *Environmental Progress & Sustainable Energy*, 42(6), e14197.

Ekinci, S. (2023). Elimination of Methylene Blue from Aqueous Medium Using an Agricultural Waste Product of Crude Corn Silk (Stylus maydis) and Corn Silk Treated with Sulphuric Acid. ChemistrySelect, 8(18), e202300284.

Güzel, F., Sayğılı, H., Sayğılı, G. A., & Koyuncu, F. (2015). New low-cost nanoporous carbonaceous adsorbent developed from carob (Ceratonia siliqua) processing industry waste for the adsorption of anionic textile dye: Characterization, equilibrium and kinetic modeling. *Journal of Molecular Liquids*, 206, 244-255.

Hasanbeigi, A., & Price, L. (2015). A technical review of emerging technologies for energy and water efficiency and pollution reduction in the textile industry. *Journal of Cleaner Production*, 95, 30-44.

Iwuozor, K. O., Ighalo, J. O., Emenike, E. C., Ogunfowora, L. A., & Igwegbe, C. A. (2021). Adsorption of methyl orange: A review on adsorbent performance. *Current Research in Green and Sustainable Chemistry*, 4, 100179.

Kahvecioğlu, K., Teğin, İ., Yavuz, Ö., & Saka, C. (2023). Phosphorus and oxygen co-doped carbon particles based on almond shells with hydrothermal and microwave irradiation process for adsorption of lead (II) and cadmium (II). *Environmental Science and Pollution Research*, 30(13), 37946-37960.

Kara, I., Tunc, D., Sayin, F., & Akar, S. T. (2018). Study on the performance of metakaolin based geopolymer for Mn (II) and Co (II) removal. *Applied clay science*, 161, 184-193.

Kaushal, S., Kaur, N., Kaur, M., & Singh, P. P. (2020). Dual-Responsive Pectin/Graphene Oxide (Pc/GO) nano-composite as an efficient adsorbent for Cr (III) ions and photocatalyst for degradation of organic dyes in waste water. *Journal of Photochemistry and Photobiology A: Chemistry*, 403, 112841.

Lima, E. C., Hosseini-Bandegharaei, A., Moreno-Piraján, J. C., & Anastopoulos, I. (2019). A critical review of the estimation of the thermodynamic parameters on adsorption equilibria. Wrong use of equilibrium constant in the Van't Hoof equation for calculation of thermodynamic parameters of adsorption. *Journal of molecular liquids*, 273, 425-434.

Liu, Q., Li, Y., Chen, H., Lu, J., Yu, G., Möslang, M., & Zhou, Y. (2020). Superior adsorption capacity of functionalised straw adsorbent for dyes and heavy-metal ions. *Journal of Hazardous Materials*, 382, 121040.

Onat, E., & Ekinci, S. (2024). A new material fabricated by the combination of natural mineral perlite and graphene oxide: Synthesis, characterization, and methylene blue removal. *Diamond and Related Materials*, 110848.

Pandey, S., & Ramontja, J. (2016). Natural bentonite clay and its composites for dye removal: current state and future potential. *American Journal of Chemistry and Applications*, 3(2), 8-19.

Sayğılı, H., Güzel, F., & Önal, Y. (2015). Conversion of grape industrial processing waste to activated carbon sorbent and its performance in cationic and anionic dyes adsorption. *Journal of Cleaner Production*, 93, 84-93.

Tamjidi, S., Esmaeili, H., & Moghadas, B. K. (2019). Application of magnetic adsorbents for removal of heavy metals from wastewater: a review study. *Materials Research Express*, 6(10), 102004.

Teğin, İ., Batur, M. Ş., Yavuz, Ö., & Saka, C. (2023). Removal of Cu (II), Pb (II) and Cd (II) metal ions with modified clay composite: kinetics, isotherms and thermodynamics studies. *International Journal of Environmental Science and Technology*, 20(2), 1341-1356.

Tural, B., Ertaş, E., & Tural, S. (2016). Removal of phenolic pollutants from aqueous solutions by a simple magnetic separation. Desalination and water treatment, 57(54), 26153-26164.

Tural, B., Ertaş, E., Enez, B., Fincan, S. A., & Tural, S. (2017). Preparation and characterization of a novel magnetic biosorbent functionalized with biomass of Bacillus Subtilis: Kinetic and isotherm studies of biosorption processes in the removal of Methylene Blue. *Journal of Environmental Chemical Engineering*, 5(5), 4795-4802

Zhul-quarnain, A., Ogemdi, I. K., Modupe, I., Gold, E., & Chidubem, E. E. (2018). Adsorption of malachite green dye using orange peel. *Journal of Biomaterials*, 2(2), 10.